MICROBIOLOGY

Prophage terminase with tRNase activity sensitizes *Salmonella enterica* to oxidative stress

Siva Uppalapati[1]†, Sashi Kant[1]†‡, Lin Liu[1], Ju-Sim Kim[1], David Orlicky[2], Michael McClelland[3], Andres Vazquez-Torres[1,4]*

Phage viruses shape the evolution and virulence of their bacterial hosts. The *Salmonella enterica* genome encodes several stress-inducible prophages. The Gifsy-1 prophage terminase protein, whose canonical function is to process phage DNA for packaging in the virus head, unexpectedly acts as a transfer ribonuclease (tRNase) under oxidative stress, cleaving the anticodon loop of $tRNA^{Leu}$. The ensuing RNA fragmentation compromises bacterial translation, intracellular survival, and recovery from oxidative stress in the vertebrate host. *S. enterica* adapts to this transfer RNA (tRNA) fragmentation by transcribing the RNA repair Rtc system. The counterintuitive translational arrest provided by tRNA cleavage may subvert prophage mobilization and give the host an opportunity for repair as a way of maintaining bacterial genome integrity and ultimately survival in animals.

Oxidative stress imposes tremendous selective pressures on all domains of life. Intracellular bacterial pathogens, such as *S. enterica,* that reside in effector cells of the mammalian innate immune system, are exposed to high concentrations of reactive oxygen species (ROS) synthesized by the respiratory burst of the phagocyte NADPH (nicotinamide adenine dinucleotide phosphate) oxidase (*1*). The cytotoxic concentrations of ROS produced by the respiratory burst damage nucleotides, metal cofactors, and sulfur-containing amino acids (*2*). Oxidation of biosynthetic enzymes induces functional auxotrophies for aromatic and branched-chain amino acids (*3*, *4*). The resulting drops in amino acids are followed by a surplus of deacylated transfer RNAs (tRNAs) that trigger an adaptation in bacteria commonly known as the stringent response (*5*–*7*). The combination of a shrinking pool of charged tRNAs together with the repression of ribosomal RNA (rRNA) and tRNA genes undermines the translational capacity of phylogenetically diverse microorganisms undergoing the stringent response during periods of oxidative stress. In this study, we describe a lysogenic prophage that represses translation in *Salmonella* exposed to oxidative stress generated by the phagocyte NADPH oxidase through the moonlighting transfer ribonuclease (tRNase) function of a deoxyribonuclease (DNase) whose canonical role is viral-genome processing and capsid packaging.

[1]University of Colorado School of Medicine, Department of Immunology and Microbiology, Aurora, CO, USA. [2]University of Colorado School of Medicine, Department of Pathology, Aurora, CO, USA. [3]Department of Microbiology and Molecular Genetics, University of California Irvine School of Medicine, Irvine, CA, USA. [4]Veterans Affairs Eastern Colorado Health Care System, Denver, CO, USA.
*Corresponding author. Email: andres.vazquez-torres@cuanschutz.edu
†These authors contributed equally to this work.
‡Present address: Bacterial Pathogenesis, Boehringer Ingelheim Animal Health USA, Ames, IA, USA.

Results

Translational halts in S. enterica after oxidative stress

To measure de novo translation in *S. enterica* in vitro in response to oxidative stress generated by application of hydrogen peroxide (H_2O_2), we used a Western blot version of SUnSET (surface sensing of translation) (*8*). *S. enterica* experienced a substantial ($P < 0.0001$) inhibition of de novo protein synthesis upon exposure to 400 μM H_2O_2 (Fig. 1, A and B). Under the high density of bacterial cultures used in these experiments, 400 μM H_2O_2 did not affect bacterial viability (Fig. 1C), indicating that *S. enterica* can tolerate moderate levels of peroxide stress by repressing translation. *S. enterica* resumed translation 90 min after exposure to H_2O_2 (Fig. 1, D and E).

To identify responses that may underlie recovery of translational activity during oxidative stress, we investigated the genome-wide transcriptional responses of *S. enterica* exposed to H_2O_2. Hierarchical clustering analysis of RNA-sequencing (RNA-seq) data revealed that 497 and 569 genes were up-regulated and down-regulated, respectively, in H_2O_2-treated *S. enterica* compared with untreated controls (fig. S1A) [false discovery rate (FDR) *P* value < 0.05; tables S1 to S4]. This analysis showed transcriptional up-regulation of *katG*, *trxC*, and *dps* of the OxyR regulon, of *mntH* and *sitABCD* involved in manganese transport, and of genes encoding the *Salmonella* pathogenicity island-2 type III secretion system, glycolysis, iron acquisition, and [Fe-S] repair. By contrast, genes encoding oxidative phosphorylation; ribosomal proteins; or the biosynthesis of lipids, amino acids, and aminoacyl tRNAs were down-regulated. Quantitative reverse transcription polymerase chain reaction (RT-PCR) confirmed the up-regulation of *katG* and *sufABC* genes and the down-regulation of oxidative phosphorylation genes (fig. S1, B and C).

The patterns of gene expression that we found are consistent with the idea that *S. enterica* adapts to oxidative stress by up-regulating antioxidant defenses, while favoring overflow metabolism and undergoing the stringent response (*2*, *5*, *9*). We also noted that the *rsr-yrlBA-rtcBA* operon, which mediates repair of fragmented RNA molecules, was up-regulated in H_2O_2-treated *S. enterica* (Fig. 1F and fig. S1D). The *rtc* operon encodes for the RNA cyclase RtcA, the RNA ligase RtcB, and the σ^{54} transcriptional activator RtcR (*10*). RtcA converts 3′ and 5′-phosphate RNA fragments to a 2′, 3′- cyclic phosphate intermediate (*11*), which serves as a substrate for the phosphodiesterase RtcB. The RtcB protein also catalyzes the GTP-driven ligation of 3′-phosphate and 5′-hydroxyl RNA fragments (*12, 13*). The activation of *rtc* genes during oxidative stress prompted us to explore the role of this operon in adaptation of *S. enterica* to the inhibition of de novo protein synthesis through oxidative stress.

Role of the RNA repair Rtc system during oxidative stress

We tested the capacity of *S. enterica rtcBA* and *rtcR* deletion mutants to synthesize protein after exposure to H_2O_2. As reported above, wild-type (WT) *S. enterica* recovered de novo protein synthesis after 90 min of H_2O_2 treatment. In comparison, the Δ*rtcBA* and Δ*rtcR* isogenic controls undergoing oxidative stress showed delayed ($P < 0.01$) de novo protein translation during the recovery phase (Fig. 2, A and B, and fig. S2, A to C). These data indicate that the RNA repair Rtc system plays a role in the adaptation of *S. enterica* to translational halts that occur during oxidative stress.

Coinciding with *rtcB* gene transcription (fig. S3A), the addition of H_2O_2 to WT *S. enterica* resulted in fragmentation of $tRNA^{Tyr}$ and $tRNA^{LeuPQTV}$ (Fig. 2, C and D), so we explored how the Rtc system aids the recovery of de novo translation through RNA repair (*10*). Further analysis revealed that *S. enterica* undergoing oxidative stress specifically experienced fragmentation of all major leucine tRNA isoacceptors $tRNA^{LeuPQTV}$, $tRNA^{LeuX}$, and $tRNA^{LeuZ}$, but not $tRNA^{Gln}$, $tRNA^{His}$, or $tRNA^{Met}$ (fig. S3B). *S. enterica* Δ*rtcBA* and Δ*rtcR* mutants experienced higher levels of $tRNA^{Leu}$ and $tRNA^{Tyr}$ fragmentation after H_2O_2 treatment than did WT controls (Fig. 2C and fig. S3C). Expression of the *rtcBA* operon in *trans* reversed the abnormally high $tRNA^{LeuPQTV}$ fragmentation of Δ*rtcBA S. enterica* after H_2O_2 treatment (fig. S3D). Sequencing of 3′ RACE products of $tRNA^{LeuPQTV}$ and $tRNA^{LeuW}$ fragments recovered from H_2O_2-treated *S. enterica* identified cleavage at positions U34 and G37 of the anticodon loop (Fig. 2E and fig. S3E).

WT and *rtc S. enterica* mutants were equally susceptible to the bacteriostatic activity of H_2O_2

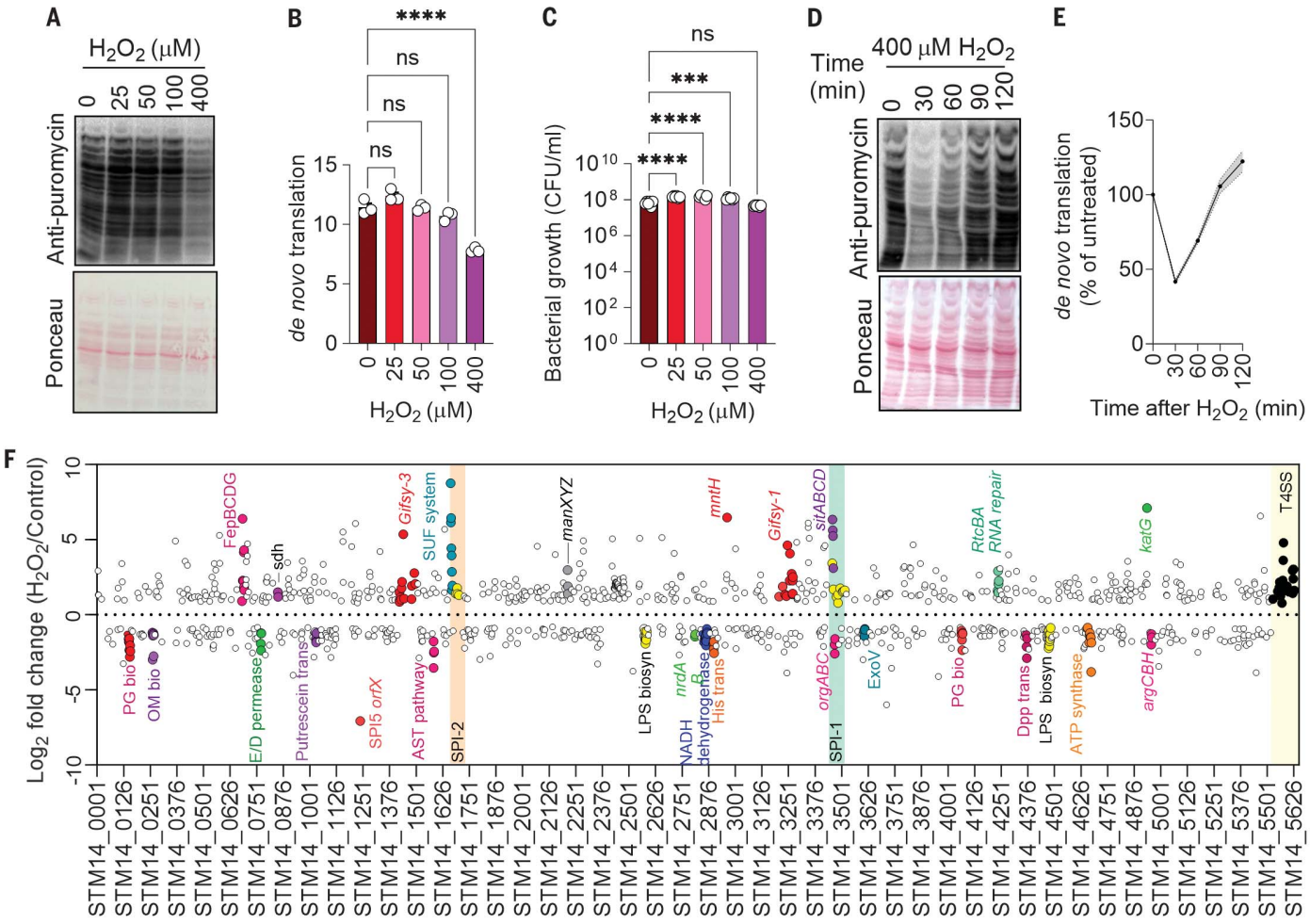

Fig. 1. Transcriptional adaptations to the repression of de novo translation in *S. enterica* undergoing oxidative stress. (**A** and **D**) Immunoblots with Ponceau S–stained controls and (**B** and **E**) a corresponding densitometric analysis examining puromycin incorporation by *S. enterica* 30 min after H_2O_2 treatment. Densitometry was normalized against Ponceau S–stained lanes with ImageJ. Data are shown as mean ± SD (n = 3 independent observations); ****$P \leq 0.0001$ as determined by one-way analysis of variance (ANOVA) with Dunnet's multiple comparison test. (**C**) Killing of *S. enterica* by H_2O_2 in PBS after 30 min of treatment. Data are shown as mean ± SD (n = 4); ****$P \leq 0.0001$ and ***$P \leq 0.001$ as determined by one-way ANOVA with Dunnet's multiple comparison test. (**F**) Differentially expressed genes in *S. enterica* after 30 min of 400 μM H_2O_2 treatment as assessed by RNA-seq (*30*). Each circle represents the average $\log_2$-fold change of four biological replicates. Genes with a $\log_2$-fold change >0.8 or <−0.8 are depicted on the top and bottom, respectively. Orange and green boxes represent pathogenicity islands, and the yellow box represents *S. enterica* plasmid genes.

(fig. S4A); however, compared with WT controls, a higher percentage ($P < 0.0001$) of Δ*rtcR* and Δ*rtcBA S. enterica* mutants were killed by H_2O_2 (Fig. 2F and fig. S4B). The Δ*rtcBA* mutant became resistant to H_2O_2 killing upon complementation with the *rtcBA* operon (fig. S4C). These data indicate that the RNA repair Rtc system protects *S. enterica* from the bactericidal effects of H_2O_2. The *rtc S. enterica* mutants were hypersusceptible to ROS produced by the respiratory burst of bone marrow–derived macrophages (Fig. 2G and fig. S4D). The Δ*rtcBA S. enterica* mutant was also attenuated in C57BL/6 mice, as measured by both a decreased competitive index when receiving intraperitoneal (i.p.) inoculation with WT controls (Fig. 2H) and the reduced burden and number of microabscesses recorded in infected livers (Fig. 2I) and spleens (fig. S4E) when inoculated as a single culture in mice. The Δ*rtcBA* mutant was also attenuated in a streptomycin-treated oral model of *S. enterica* infection (fig. S4F). The Δ*rtcBA S. enterica* strain was as fit as WT *S. enterica* in *Cybb*$^{-/-}$ mice lacking the catalytic gp91*phox* subunit of the phagocyte NADPH oxidase (Fig. 2, H and I, and fig. S4E). Cumulatively, these experiments show that the RNA repair Rtc system assists *S. enterica* to adapt to ROS cytotoxicity in macrophages and mice.

tRNA fragmentation after SOS induction of a temperate prophage

We sought the molecular mechanism underlying the cleavage of tRNAs in *S. enterica* after H_2O_2 treatment. Gene expression in *S. enterica* exposed to H_2O_2 showed that the SOS response was activated (Fig. 3A) (*10*, *14*). Thus, we examined tRNA fragmentation in a strain lacking the SOS recombinase RecA that facilitates DNA repair after oxidative damage. The Δ*recA S. enterica* mutant did not accumulate 5′-$tRNA^{Leu}$ fragments upon H_2O_2 treatment (Fig. 3B), indicating that cleavage of $tRNA^{Leu}$ in *S. enterica* undergoing oxidative stress is induced by the SOS response. Transcription of RNA repair *rtc* genes was not activated in the Δ*recA* mutant, probably because of the lack of tRNA fragments that are recognized by the RtcR regulatory protein (Fig. 3C). Together, these results indicate that the RNA repair Rtc system provides protective feedback to the tRNA fragmentation unleashed in response to ROS-mediated genotoxicity.

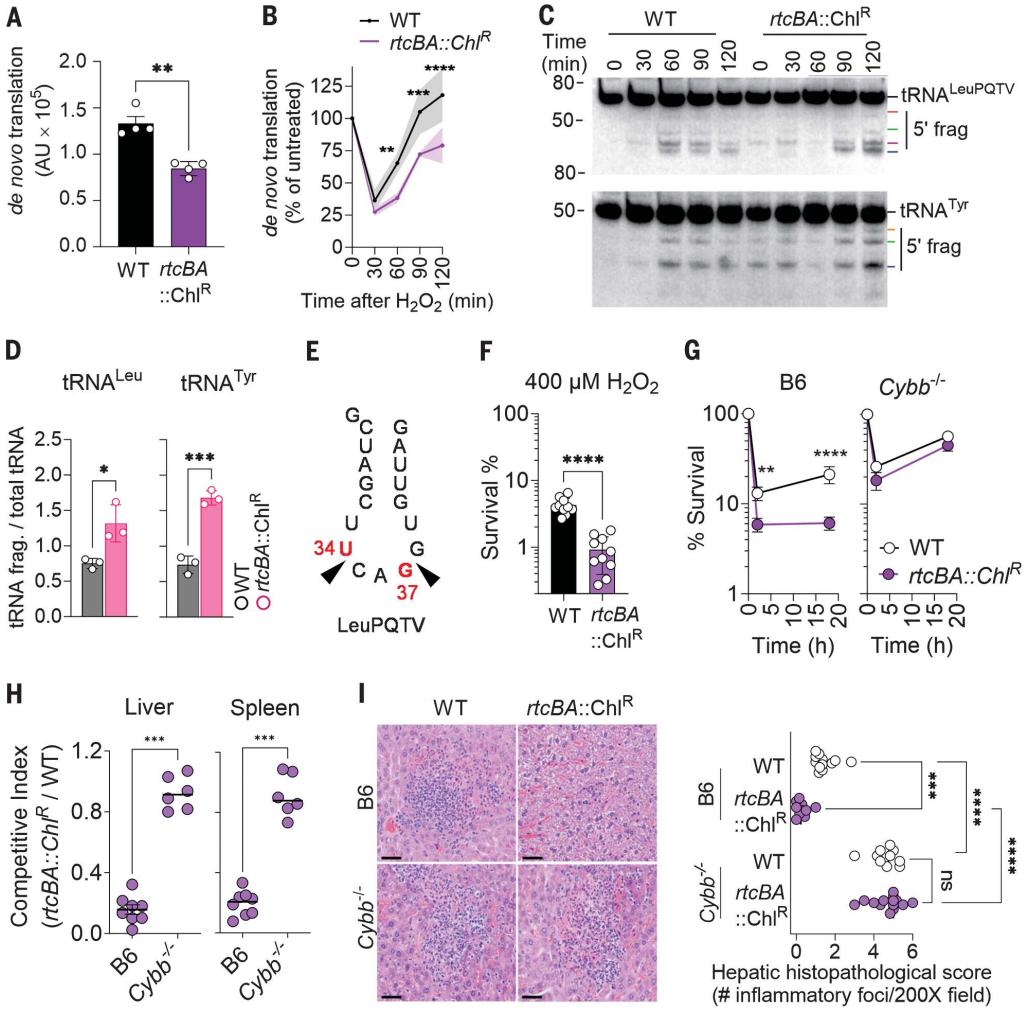

Fig. 2. Repair of tRNA by the RNA repair Rtc system protects *S. enterica* from the phagocyte NADPH oxidase. Densitometry (**A** and **B**) of the puromycin^{+} proteome in WT and *rtc* mutants. Specimens in (B) were treated with 400 μM H_2O_2. Data are shown as mean ± SD (n = 4). (**C**) tRNA fragmentation was visualized by Northern blotting in *S. enterica* after 5 mM H_2O_2 treatment. (**D**) Densitometry of tRNA fragments 2 hours after H_2O_2 treatment, corresponding to data in (C). Data are shown as mean ± SD (n = 3). (**E**) Position of tRNA^{LeuPQTV} cleavage in H_2O_2-treated *S. enterica* as assessed by sequencing and 3′ RACE. (**F**) Killing of *S. enterica* after 2 hours of treatment with 400 μM H_2O_2 in phosphate-buffered saline (PBS). Data are shown as mean ± SD (n = 10). (**G**) Intracellular survival of *S. enterica* in bone marrow–derived macrophages from C57BL/6 (B6) and *Cybb*$^{-/-}$ mice. Data are shown as mean ± SD (n = 6). (**H**) Competitive index of *S. enterica* in livers and spleens of C57BL/6 (B6) and *Cybb*$^{-/-}$ mice 3 days after i.p. inoculation with equal numbers of WT and *ΔrtcBA S. enterica* (n = 6 to 7). (**I**) Histopathology of paraffin-embedded, hematoxylin and eosin (H&E)–stained liver tissues isolated 3 days after infection. Scale bars, 50 μm. The panel on the right shows the average number of microabscesses and necrotic foci per 200X field of liver tissue stained with H&E (n = 6 to 7). *$P \le 0.05$, **$P \le 0.01$, ***$P < 0.001$, and ****$P < 0.0001$ as determined by Student's t test [(A), (D), and (F)], Mann-Whitney test (G), one-way ANOVA with Dunnet's multiple comparison test (B), or two-way ANOVA (H).

The transcriptional analysis showed that *S. enterica* undergoing oxidative stress also increased transcription of Gifsy-1 and Gifsy-3 prophage genes (Fig. 1F). As it appears that oxidative DNA damage activates prophage simultaneously with RNA repair (*15*), we investigated whether Gifsy prophage activation caused tRNA cleavage. A strain of *S. enterica* lacking all three Gifsy prophages failed to induce tRNA^{Leu} cleavage after exposure to H_2O_2 (Fig. 3D). Endoribonuclease activity was mapped to the Gifsy-1 prophage. Gifsy-1–deficient *S. enterica* failed to induce tRNA^{Leu} cleavage upon H_2O_2 treatment (Fig. 3E and fig. S5A) and sustained higher translation but lower *rtcA* transcription after H_2O_2 treatment than did WT bacteria (Fig. 3, F and G). Treatment of *Salmonella* with 5 mM H_2O_2 for 2 hours did not activate the Gifsy-1 lytic cycle as measured by the absence of plaque-forming particles in culture supernatants or by RT-PCR of circularized DNA from the prophage (fig. S5B). These findings suggest that the expression of the Gifsy-1 tRNase activity is not reliant on phage replication. Gifsy-1–deficient *S. enterica* were not only more resistant to H_2O_2 killing than were WT controls (Fig. 3H) but were also at a competitive advantage in C57BL/6 mice when tested in competition with WT *S. enterica* (Fig. 3I). The presence of the Gifsy-1 prophage reduced resistance of *S. enterica* to oxidative stress but attenuated *S. enterica* virulence in *Cybb*$^{-/-}$ mice lacking the phagocyte NADPH oxidase. Thus, in the context of oxidative stress created by the respiratory burst of phagocytic cells, the Gifsy-1 prophage sensitizes *S. enterica* to oxidative killing. However, the Gifsy-1 prophage provides advantages to *Salmonella* at times when phagocyte NADPH oxidase is not expressed, as evidenced by the disadvantage of the ΔGifsy-1 strain in *Cybb*$^{-/-}$ mice (Fig. 3I).

Cleavage of tRNA by Gifsy-1 terminase during oxidative stress

The data so far indicated the presence of a previously uncharacterized nuclease in the Gifsy-1 prophage that can target its bacterial host's tRNA molecules. We initially focused on the STM14_3218-20 operon within the Gifsy-1 prophage, a locus that is associated with the activation of *rtc* gene transcription after antibiotic-mediated DNA damage (*15*) and that is present in *Salmonella* Typhimurium strain 14028s but absent in *S.* Typhimurium strains LT2 or SL1344. Northern blot analyses showed that H_2O_2 induced tRNA^{Leu} cleavage in *S.* Typhimurium strains LT2, SL1344—as well as in *S.* Typhimurium 14028s mutants bearing multiple- or single-gene deletions in the STM14_3218-20 operon—as efficiently as in the WT 14028s strain (fig. S5, C and D). Collectively, these findings suggest that the nuclease responsible for tRNA cleavage in H_2O_2-treated *S. enterica* maps to a locus encoded outside of the STM14_3218-20 operon. Neither the *dinJ* or *yafQ* genes encoded proximal to the *rtc* operon were required for H_2O_2-induced fragmentation of tRNA^{Leu} (fig. S5D), indicating that the RNase encoded in this putative toxin-antitoxin system was not involved.

Systematic mapping of the Gifsy-1 genome (Fig. 4A) associated a gene in the capsid- and DNA-packaging region with cleavage of *S. enterica* $tRNA^{Leu}$ during oxidative stress (Fig. 4B and fig. S6, A and B). The terminase encoded in the Gifsy-1 *gpA* gene is the only determinant in the capsid- and DNA-packaging region that has canonical endonuclease activity. Terminases hydrolyze linear concatemers of double-stranded viral DNA into single genomes ready for packaging into mature virions. The combination of phylogenetic analysis and the AlphaFold structure of the C-terminal domain of the Gifsy-1 GpA revealed intriguing similarities between this terminase and colicin family members (Fig. 4C and fig. S6C), some of which are endoribonucleases with specificity against the anticodon loop of tRNA molecules (*16*). Deletion of the *gpA* gene from Gifsy-1 averted $tRNA^{Leu}$ fragmentation after exposure of *S. enterica* to H_2O_2 (Fig. 4D), a phenotype that could be complemented with the *gpA* gene in *trans* (fig. S6D). Cumulatively, these findings support the role of Gifsy-1 terminase in tRNA cleavage after oxidative stress.

To further test the idea that the Gifsy-1 terminase has endoribonuclease activity, we expressed the GpA protein with an arabinose-inducible promoter. In the absence of H_2O_2, induction of the *gpA* gene in *S. enterica* did not result in fragmentation of tRNA (fig. S7A). However, heterologous expression of *gpA* simultaneously with the addition of 400 μM H_2O_2 resulted in the fragmentation of $tRNA^{Leu}$ (Fig. 4E). These findings suggest that oxidative stress either promotes endoribonuclease activity in the GpA terminase or that the tRNA cleavage is the result of the synergistic actions of GpA with another factor induced by oxidative stress. In support of the former model, recombinant GpA treated with H_2O_2—but not GpA treated with dithiothreitol (DTT)—induced cleavage of $tRNA^{Leu}$ in a reconstituted biochemical system (Fig. 4F and fig. S7B). The tRNase activity of the oxidized recombinant GpA was potentiated by the addition of ATP in the reactions (fig. S7C) and resulted in 3′-phosphate or 2′, 3′ cyclic phosphate and 5′-hydroxyl fragments amenable for RtcB repair (fig. S7D). The oxidized GpA protein retained the canonical DNase activity (fig. S7E). Reduced and oxidized recombinant GpA differentially migrated in non-reducing SDS gels (fig. S7F), indicating that the Gifsy-1 GpA terminase is redox active. Recombinant GpA preparations further purified by size-exclusion chromatography retained tRNase activity upon oxidation (fig. S7, G to I), demonstrating that the tRNase activity maps to GpA. Recombinant GpA cleaved $tRNA^{LeuPQTV}$ at the G37 wobble position in the anticodon loop (Fig. 4G and fig. S7J). Our bioinformatic analysis of the projected AlphaFold structure of the C-terminal domain of GpA revealed a Walker A motif close to the predicted colicin tRNase domain (Fig. 4H). Mutagenesis of Lys^{497} and His^{481} in the Walker A motif and predicted tRNase domain, respectively, prevented cleavage of both $tRNA^{LeuPQTV}$ and a DNA template containing the *cosN* site by the oxidized GpA protein (Fig. 4I and fig. S7, K to M). Hence, the oxidized form of the redox-sensitive GpA Gifsy-1 terminase can moonlight as a tRNase with specificity to the anticodon loop without losing its canonical DNase activity.

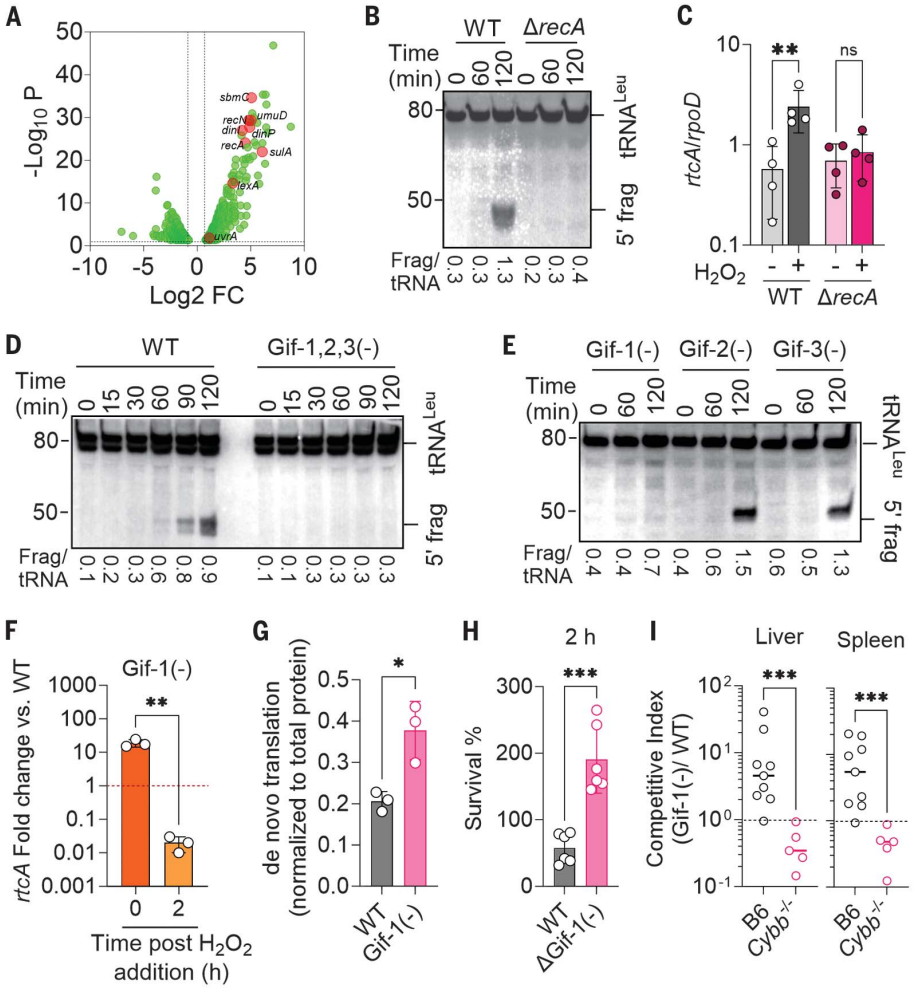

Fig. 3. The SOS response activates prophage-dependent tRNA cleavage in *S. enterica* undergoing oxidative stress. (**A**) Differentially expressed genes (DEGs) in WT *S. enterica* after treatment with 400 μM H_2O_2. DEGs were identified by DESeq2 and edgeR with tagwise dispersion and FDR-corrected *P* values. (**B**, **D**, and **E**) $tRNA^{LeuPQTV}$ fragments were visualized by Northern blotting in log-phase *S. enterica* after treatment with 5 mM H_2O_2. Densitometric quantification of 5′ /intact tRNA is presented below each lane. (**C** and **F**) *rtcA* transcription in log-phase *S. enterica* 1 hour after treatment with 400 μM H_2O_2 or PBS. Cycle threshold values were normalized to the *rpoD* housekeeping gene. Data are shown as mean ± SD [(C), *n* = 4; (F), *n* = 3]. $^{**}P < 0.01$ as determined by unpaired Mann-Whitney test. Transcription in (F) is expressed relative to WT controls. (**G**) Densitometry of the de novo translated proteome as assessed by puromycin incorporation in the indicated *S. enterica* strains grown in MOPS-GLC media and treated with 400 μM H_2O_2 for 2 hours. Data are shown as mean ± SD (*n* = 3); $^{*}P \leq 0.05$ as determined by Student's *t*-test. (**H**) Antimicrobial activity of H_2O_2 on *S. enterica* 2 hours after treatment. Data are shown as mean ± SD (*n* = 6); $^{****}P \leq 0.0001$ as determined by one-way ANOVA with Dunnet's multiple comparison test. (**I**) Competitive index of *S. enterica* in livers and spleens of C57BL/6 (B6) and *Cybb*$^{-/-}$ mice 3 days after i.p. inoculation of equal numbers of WT and Gifsy-1–deficient *S. enterica* (*n* = 5 to 8). $^{***}P < 0.001$ as determined by Mann-Whitney test.

A strain of *S. enterica* lacking the Gifsy-1 *gpA* gene was hyperresistant to H_2O_2 and hypervirulent in C57BL/6 mice when tested in oral and systemic models of infection (Fig. 4, J and K, and fig. S8A). The expression of *gpA* in *trans* reversed the hypersusceptibility of the Δ*gpA* mutant to H_2O_2 (fig. S8B). Moreover, the presence of a functional *gpA* gene slowed the recovery of de novo protein translation after peroxide stress (fig. S8, C and D). These

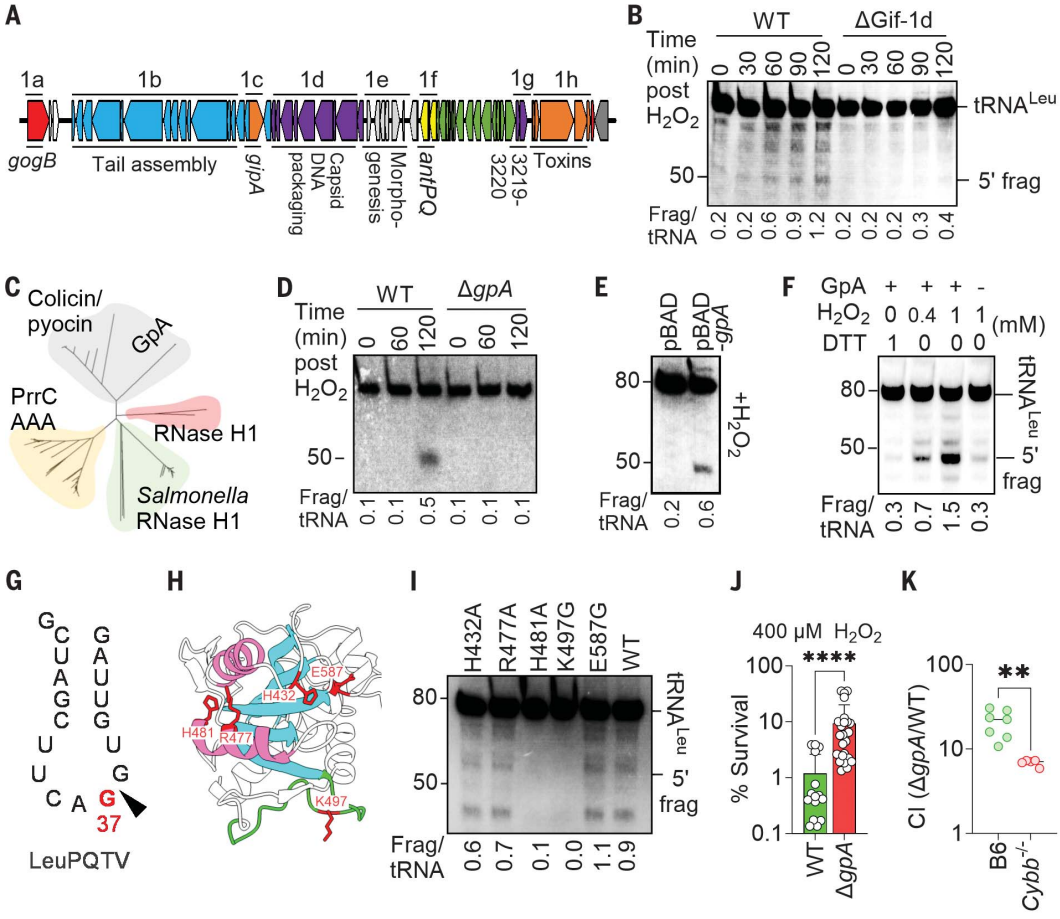

Fig. 4. Gifsy-1 terminase cleaves tRNA in *S. enterica* during oxidative stress. (**A**) Genomic organization of Gifsy-1 region in *S. enterica* 14028s. (**B**, **D**, and **E**) $tRNA^{LeuPQTV}$ fragments were visualized by Northern blotting in *S. enterica* grown to log phase in LB broth and treated with 5 mM H_2O_2. Strains in (E) expressing pBAD or pBAD-*gpA* were treated with 500 μM H_2O_2. (**C**) Phylogenetic tree of full-length *S. enterica* GpA and known ribonucleases. (**F** and **I**) Total RNA extracted from log-phase *S. enterica* was treated with recombinant GpA proteins. Recombinant GpA variants in (I), and where indicated in (F), were treated with H_2O_2. $tRNA^{LeuPQTV}$ fragments were visualized with Northern blot. Densitometric quantification of 5′ fragment and intact tRNA is presented below each lane. Single-letter abbreviations for the amino acid residues are as follows: A, Ala; E, Glu; G, Gly; H, His; K, Lys; R, Arg. In the mutants, other amino acids were substituted at certain locations; for example, H432A indicates that histidine at position 432 was replaced with alanine. (**G**) Site of cleavage of $tRNA^{LeuPQTV}$ by H_2O_2-treated recombinant GpA protein was determined by 3′ RACE and sequencing. (**H**) AlphaFold representation of the C-terminal nuclease domain of GpA. Walker A motif is in green, whereas α helices and β sheets of the predicted nuclease site are in pink and cyan, respectively. Residues mutated in (I) are shown in red. (**J**) Survival of *S. enterica* grown overnight in LB broth and treated for 2 hours with 400 μM H_2O_2 in PBS. Data are shown as the mean ± SD (n = 16 to 26). (**K**) Competitive index of *S. enterica* in livers of C57BL/6 (B6) and *Cybb*$^{-/-}$ mice 3 days after i.p. inoculation of equal numbers of WT and Δ*gpA S. enterica* (n = 5 to 7). $^{**}P < 0.01$ and $^{****}P \leq 0.0001$ as determined by Mann-Whitney test [(J) and (K)].

findings indicate that when acting as an RNAse, the prophage GpA protein predisposes *S. enterica* to oxidative stress generated in the innate host response.

Discussion

The pathogenesis of *Vibrio cholerae*, enterohemorrhagic *Escherichia coli*, *Shigella dysenteriae*, or *Clostridium botulinum* is intimately linked to the toxins encoded within their temperate bacteriophages (*17*). The virulence of *S. enterica* has also been chiseled by the horizontal acquisition of prophages. The Gifsy-2 prophage promotes *S. enterica* virulence through vacuolar remodeling by an effector of the pathogenicity island-2 type III secretion system and the antioxidant properties of a Cu/Zn superoxide dismutase (*18*, *19*). In contrast to the archetypical lysogenic bacteriophages that provide virulence traits to their bacterial hosts, our investigations show that the Gifsy-1 prophage reduces fitness of *S. enterica* in the context of ROS-induced oxidative stress produced by phagocyte NADPH oxidase in mice. Thus, the redox-responsive terminase encoded in the capsid- and DNA-packaging region of the Gifsy-1 prophage gains endoribonuclease activity upon oxidation, sensitizing *S. enterica* to oxidative killing.

ROS damage almost every cogwheel of the translational machinery, including ribosomes, elongation factors, mRNA, tRNA, and tRNA synthetases [reviewed in (*20*)]. ROS oxidize cysteine and methionine residues in small (S17) and large (L7/L12, L14) ribosomal subunit proteins and damage ribonucleotides that can then be misincorporated into the transcriptome (*21*–*23*). Moreover, the [4Fe-4S] cluster of the *ilvD*-encoded dihydroxyacid dehydratase in the biosynthesis of branched-chain amino acids is especially vulnerable to the toxic effects of ROS (*24*–*26*). Cleavage of $tRNA^{Leu}$ isoacceptors should be included in the mechanism by which oxidative stress negatively impacts translation in *S. enterica*. In contrast to the direct damage caused by ROS to ribosomes, biosynthetic enzymes, and ribonucleotides, the cleavage of tRNA under oxidative stress is an indirect result of the SOS-mediated expression of the Gifsy-1 terminase. Because about 20% of all codons in the genome of *S. enterica* encode for leucine residues, the concerted effects of oxidative stress on dehydroxyacid dehydratase and the $tRNA^{Leu}$ cleavage mediated by Gifsy-1 terminase will have a profound effect on the nascent proteome (fig. S8).

The importance of the RNA repair Rtc system in resistance of *S. enterica* to the phagocyte NADPH oxidase indicates that this intracellular pathogen benefits from recycling damaged tRNA. Given the complex modifications involved in maturation of tRNAs (*27*), with most concentrated at the wobble position of the anticodon stem loop, de novo tRNA generation during oxidative stress must be taxing to an already energy- and resource-constrained cell. Recycling of damaged tRNA molecules becomes critical in the resistance of *S. enterica* to oxidative stress as shown by the *Cybb*-dependent attenuation of *rtc* mutants.

Why would a pathogen maintain an apparently debilitating locus within its genome?

A possible answer to this paradox might lie in the fact that prokaryotic cells couple transcription and translation. The induction of Gifsy-1–mediated tRNA cleavage through the SOS response in *S. enterica* suggests that the observed halts in translation are caused by double-stranded DNA damage. The concerted inhibition of leucine biosynthesis and cleavage of $tRNA^{Leu}$ must slow ribosomes through the nascent transcript. Decelerating ribosomes permits backtracking of RNA polymerase (*28*), which would enable access of repair enzymes to DNA lesions (*29*). Therefore, Gifsy-1–mediated inhibition of translation in H_2O_2-treated *S. enterica* may help maintain the integrity of the genome. In this context, *S. enterica* may hijack host cell–derived ROS to activate a lysogenic phage determinant that halts bacterial translation and growth during intense periods of oxidative stress, providing opportunities for repair and survival. In addition, the moonlighting tRNase function of GpA precludes phage-genome processing and capsid maturation, protecting the bacterial host from the lytic cycle at times of exposure to oxidative stress exerted by the innate immune response.

REFERENCES AND NOTES

1. P. Mastroeni *et al*., *J. Exp. Med.* **192**, 237–248 (2000).
2. F. C. Fang, *Nat. Rev. Microbiol.* **2**, 820–832 (2004).
3. S. Jang, J. A. Imlay, *J. Biol. Chem.* **282**, 929–937 (2007).
4. B. Ezraty, A. Gennaris, F. Barras, J. F. Collet, *Nat. Rev. Microbiol.* **15**, 385–396 (2017).
5. J. S. Kim *et al*., *Proc. Natl. Acad. Sci. U.S.A.* **115**, E11780–E11789 (2018).
6. L. E. Leiva *et al*., *Front. Genet.* **11**, 856 (2020).
7. V. N. Fritsch *et al*., *Free Radic. Biol. Med.* **161**, 351–364 (2020).
8. C. A. Goodman, T. A. Hornberger, *Exerc. Sport Sci. Rev.* **41**, 107–115 (2013).
9. S. Chakraborty *et al*., *Nat. Commun.* **11**, 1783 (2020).
10. K. J. Hughes, X. Chen, A. M. Burroughs, L. Aravind, S. L. Wolin, *Cell Rep.* **33**, 108527 (2020).
11. U. Das, S. Shuman, *RNA* **19**, 1355–1362 (2013).
12. M. R. Manwar *et al*., *Sci. China Life Sci.* **63**, 251–258 (2020).
13. H. Temmel *et al*., *Nucleic Acids Res.* **45**, 4708–4721 (2017).
14. C. A. Juan, J. M. Pérez de la Lastra, F. J. Plou, E. Pérez-Lebeña, *Int. J. Mol. Sci.* **22**, 4642 (2021).
15. J. E. Kurasz *et al*., *J. Bacteriol.* **205**, e0026222 (2023).
16. K. Tomita, T. Ogawa, T. Uozumi, K. Watanabe, H. Masaki, *Proc. Natl. Acad. Sci. U.S.A.* **97**, 8278–8283 (2000).
17. P. L. Wagner, M. K. Waldor, *Infect. Immun.* **70**, 3985–3993 (2002).
18. M. A. De Groote *et al*., *Proc. Natl. Acad. Sci. U.S.A.* **94**, 13997–14001 (1997).
19. T. D. Ho *et al*., *J. Bacteriol.* **184**, 5234–5239 (2002).
20. M. Fasnacht, N. Polacek, *Front. Mol. Biosci.* **8**, 671037 (2021).
21. N. Shcherbik, D. G. Pestov, *Cells* **8**, 1379 (2019).
22. C. L. Simms, B. H. Hudson, J. W. Mosior, A. S. Rangwala, H. S. Zaher, *Cell Rep.* **9**, 1256–1264 (2014).
23. L. I. Leichert *et al*., *Proc. Natl. Acad. Sci. U.S.A.* **105**, 8197–8202 (2008).
24. D. H. Flint, J. F. Tuminello, M. H. Emptage, *J. Biol. Chem.* **268**, 22369–22376 (1993).
25. L. Macomber, J. A. Imlay, *Proc. Natl. Acad. Sci. U.S.A.* **106**, 8344–8349 (2009).
26. L. Yang *et al*., *Proc. Natl. Acad. Sci. U.S.A.* **116**, 14368–14373 (2019).
27. V. de Crécy-Lagard, M. Jaroch, *Trends Microbiol.* **29**, 41–53 (2021).
28. S. Proshkin, A. R. Rahmouni, A. Mironov, E. Nudler, *Science* **328**, 504–508 (2010).
29. B. K. Bharati *et al*., *Nature* **604**, 152–159 (2022).
30. S. Kant *et al*., *PLOS Biol.* **21**, e3002051 (2023).
31. S. Uppalapati *et al*., Data from: Prophage terminase with tRNase activity sensitizes S. enterica to oxidative stress, Dryad (2024); https://doi.org/10.5061/dryad.xpnvx0knt.

ACKNOWLEDGMENTS

We thank J. Jones-Carson for kindly providing the mice. We thank J. Hesselberth for technical discussions on tRNA Northern blotting and for helpful discussions with the manuscript. We thank H. V. Batra for valuable discussions on protein expression and purification. We also thank A. Margolis for comments on the manuscript, and we thank the Mass Spectrometry Proteomics Shared Resource Facility, University of Colorado Anschutz Medical Campus, for protein identification. **Funding:** This work was supported by VA Merit Grants BX0002073 and IK6BX005384 and by NIH grants R01AI54959 and R01AI136520. M.M. was funded in part by NIH grant R03AI139557. **Author contributions**: Conceptualization: S.U. and A.V.T. Data curation: S.U., L.L., S.K., D.O., and A.V.T. Formal analysis: S.U., L.L., S.K., D.O., and A.V.T. Funding acquisition and resources: A.V.T. and M.M. Investigation: S.U., L.L., S.K., D.O., and A.V.T. Methodology: S.U., L.L., S.K., and D.O. Supervision and validation: J.S.K. and A.V.T. Writing – original draft, review, and editing: S.U. and A.V.T. **Competing interests**: The authors declare that they have no competing interests. **Data and materials availability:** All data needed to evaluate the conclusions in the paper are present in the paper and/or in the supplementary materials. RNA-seq data are available in the GEO database under accession no. GSE203342. Bacterial cultures and plasmids generated in the study are available upon request to the corresponding author. All the data and unprocessed images utilized to draw figures in the manuscript are available at Dryad (*31*).

SUPPLEMENTARY MATERIALS

science.org/doi/10.1126/science.adl3222
Materials and Methods
Figs. S1 to S9
Tables S1 to S7
References (*32*–*39*)
MDAR Reproducibility Checklist

Submitted 11 October 2023; accepted 28 February 2024
10.1126/science.adl3222